Activation of Npas1-neurons in the Ventral Pallidum Mediates Stress Susceptibility

Gessynger Morais-Silva[1,2,3,*]; Hyungwoo Nam[1,*]; Rianne Campbell[1], Mahashweta Basu[4,5] Marco Pagliusi Jr[1,6]; Megan E Fox[1,7], Savio Chan[8]; Sergio D Iñiguez[9], Seth Ament[4,5], Marcelo Tadeu Marin[2,3]; Mary Kay Lobo[1,#]

1. Department of Anatomy and Neurobiology, University of Maryland School of Medicine, Baltimore, MD, USA.
2. Sao Paulo State University (UNESP), School of Pharmaceutical Sciences, Laboratory of Pharmacology, Araraquara, SP, Brazil.
3. Joint Graduate Program in Physiological Sciences, UFSCar/UNESP, São Carlos/Araraquara, SP, Brazil.
4. Department of Psychiatry, University of Maryland School of Medicine, Baltimore, MD, USA.
5. Institute for Genome Sciences, University of Maryland School of Medicine, Baltimore, MD, USA.
6. Department of Structural and Functional Biology, State University of Campinas, Campinas, SP, Brazil.
7. Current address - Department of Anesthesiology, Pennsylvania State College of Medicine, Hershey, PA, USA
8. Department of Neuroscience, Northwestern University, Chicago, IL, USA.
9. Department of Psychology, University of Texas at El Paso, El Paso, TX, USA

*These authors contributed equally

Corresponding author:
Dr. Mary Kay Lobo, PhD
Department of Anatomy and Neurobiology
University of Maryland School of Medicine
20 Penn Street, HSFII Rm 265
Baltimore, MD 21201, USA
E-mail: mklobo@som.umaryland.edu

Running title: VP activity underlies stress susceptibility

Abstract

Background: Altered activity of the ventral pallidum (VP) underlies disrupted motivation after stress exposure. The VP is a very heterogeneous structure comprised of many different neuron types with distinct electrophysiological properties and projections. Neuronal PAS 1-positive (Npas1+) VP neurons are thought to send projections to brain regions critical for stress response. In this study, we evaluated how activity of VP Npas1+ neurons affect emotional behaviors and responses to social stress.

Methods: We used a chemogenetic approach to manipulate VP Npas1+ neurons during social defeat stress (SDS) and behavioral tasks related to anxiety and motivation in Npas1-Cre mice. We employed a similar approach in females using the chronic witness defeat stress (CWDS). Finally, to characterize VP Npas1+ neuron circuitry and molecular identity we evaluated the projection targets of the VP Npas1+ neurons and performed RNA-seq on ribosome-associated mRNA from VP Npas1+ neurons.

Results: Chemogenetic activation of VP Npas1+ neurons increased susceptibility to a subthreshold (S)SDS and anxiety-like behavior in the elevated plus maze and open field. Inhibition of VP Npas1+ neurons enhanced resilience to chronic (C)SDS and CWDS. We identified VP Npas1+ projections to the nucleus accumbens (NAc), ventral tegmental area (VTA), medial and lateral habenula (LHb), lateral hypothalamus (LH), thalamus, medial and lateral septum, and periaqueductal gray area. VP Npas1+ neurons displayed distinct transcriptomes representing distinct biological processes.

Conclusions: Activity, of VP Npas1+ neurons, modulates susceptibility to social stressors and anxiety-like behavior. These outcomes could be related to their projections to brain regions that modulate reward and aversion.

Keywords: depression; ventral pallidum; Npas1; social defeat stress; DREAADs.

Introduction

Mood disorders, which include symptoms of anhedonia and disrupted motivation, are strongly associated with the brain's reward circuitry (1). Evidence suggest that disruptions in reward circuitry, widely known for their role in substance use disorder, are implicated in the etiology of depression and treatment inefficacy (2,3).

The ventral pallidum (VP) is an important structure within the reward circuitry that has a prominent role in the processing of reward information and execution of motivated behaviors (4,5). This is a unique structure as it contains both hedonic hotspots and coldspots, spatially distinct groups of neurons in which opioid neurotransmission can increase (hotspots) or decrease (coldspots) hedonic value of a given reinforcer and motivation (6). From a circuit standpoint, VP is a structure that is closely connected to the ventral tegmental area (VTA) and the nucleus accumbens (NAc), which are two of the best-characterized areas of the reward circuitry. VP neurons also project to aversive centers such as lateral habenula (LHb). These circuit features make VP a key structure for encoding hedonic value and control of motivated and aversive behaviors (7,8). Thus, it is not surprising that altered VP activity is shown to affect both anhedonia and social aversion (9). Specifically, pharmacogenetic and optogenetic inhibition of VP parvalbumin-positive neurons (PV+ neurons) projecting to VTA or LHb has been shown to improve depressive-like behaviors in mice (10). In humans, atrophy or lesions in the pallidal regions are related to depression symptoms such as anhedonia and social withdrawal (11–14), and VP serotonin binding is reduced in depressed patients (15).

The VP is a highly heterogeneous brain area, comprised of diverse neuronal phenotypes and innervated by numerous brain areas that release various types of neurotransmitters (4), and intrinsically implicated in its role of controlling complex behaviors such as motivation and aversion. The NAc is the major input source, innervating the VP with GABAergic and peptidergic synapses (from both D1 and D2 medium spiny neurons), which primarily target pallidal GABAergic and, to a lesser extent, cholinergic neurons (4,16). The VP neurons also send projections back to the NAc, which are classically known to be GABAergic (17,18). Dopaminergic projections to the VP arise mainly from the VTA (19,20), which also send glutamatergic and GABAergic signals (21,22). Interestingly, VTA dopaminergic neurons that send projections to the VP often co-express enzymes related to glutamate synapses (21). Both GABAergic and glutamatergic projections from the VP to the VTA are described, while only glutamatergic projections are reported in the VP to LHb connections (10,23). Another feature that distinguishes VP→VTA to VP→LHb projection neurons is their axonal branching pattern, where VP axons projecting to VTA collateralize to the lateral hypothalamus while VP axons to LHb send collaterals to the medial thalamic nucleus (24).

The Npas1 (Neuronal PAS 1) protein is a transcriptional repressor that has been demonstrated to play an important role in neuronal differentiation (25). It is increased in the brain of rodent embryos and reaches stable levels after the maturation of the nervous system (26). In the globus pallidus (GP), the Npas1-positive (Npas1+) neurons are a distinct class of neurons from the more abundant PV+ neurons (27–29) and they strongly project to striatal regions (30). They also receive inputs from diverse brain

regions related to stress response, especially from the central amygdala (31). Although the Npas1+ neurons in the VP have not been characterized yet, similarities between the GP and VP can be useful for understanding the properties of these cells in the VP.

Given the pivotal role of the VP in motivated behaviors and its anatomical position, receiving inputs from and sending projections to diverse areas involved in the expression of behaviors related to stress and motivation, the activity of the VP Npas1+ neurons are likely important to the development of behavioral alterations related to stress exposure. Thus, our current work aims to evaluate the role of VP Npas1+ neuronal activity on the susceptibility to social stress and in emotion-related behaviors.

Material and methods

Animals

All procedures regarding animal use in this study were approved by the University of Maryland School of Medicine (UMSOM) Institutional Animal Care and Use Committee. Mice were given food and water *ad libitum* and housed in UMSOM animal facilities on a 12:12 h light/dark cycle (experiments performed during the light-phase).

Npas1-Cre-2A-tdTomato hemizygotes (Npas1-Cre) and Npas1-Cre-2A-tdTomato-RiboTag (Npas1-Cre-RT) mice were used as experimental mice. The Npas1-Cre strain was generated as previously described (27) on a C57BL/6 background. Npas1-Cre-RT mice were generated by breeding Npas1-Cre mice with RiboTag $(RT)^{+/+}$ mice ($Rpl22^{tm1.1Psam/J}$) (32) on a C57BL/6 background. Male CD-1 retired breeders (Charles River, >4 months) were used as aggressors in social defeat stress experiments. Experimental mice were 8 weeks of age at the time of viral injections.

Drugs

Clozapine-N-oxide (CNO, Cayman Chemical, Ann Arbor, MI, US) was used to activate the designer receptors exclusively activated by designer drugs (DREADDs), diluted in saline (0.1 mg/mL) and injected in a dose of 1 mg/kg (0.1 mL/10 g, i.p.).

Viral vectors and stereotaxic surgery

Adeno-associated viruses (AAVs) with a double inverted open reading frame containing the excitatory DREADD fused to mCherry hM3D(Gq)-mCherry (AAV5-hSyn-

DIO-hM3Dq-mCherry, Addgene plasmid #44362, Watertown, MA, USA) or the inhibitory DREADD fused to mCherry hM4D(Gi)-mCherry (AAV5-hSyn-DIO-hM4Di-mCherry, Addgene plasmid #44361) were used for chemogenetic manipulation of Npas1+ neurons. AAV5-hSyn-DIO-eYFP (UNC Vector Core Facility, Chapel Hill, NC, USA) was used in control groups, and the animals used for tracing of projection targets.

For viral infusions, mice were anesthetized with isoflurane (3% induction, 1.5% maintenance) and had their head fixed in a stereotaxic (Kopf Instruments, Tujunga, CA, USA) for targeting of the VP bilaterally (anteroposterior, +0.9 mm; mediolateral, ±2.2 mm; dorsoventral, -5.3 mm from the Bregma). The virus (300 nL) was infused with 33-gauge Neuros syringes (Hamilton Co., Reno, NV, USA) at a rate of 0.1 µL/min, and the needle was left in place for 12 min following the infusion. Mice were allowed to recover for 2 weeks before the beginning of the experiments.

Social defeat stress (SDS)

Social defeat stress was performed as previously by our lab (33–36) using a well-established protocol (37). Briefly, experimental mice were placed in hamster cages with perforated clear dividers containing an aggressive resident mouse (retired CD1 breeder). In chronic SDS (CSDS), mice were physically attacked by a resident for 10 min, then housed opposite the resident on the other side of the divider for 24 h sensory interaction. The defeat session was repeated with a novel resident each day for 10 consecutive days. For subthreshold SDS (SSDS) (33–35) experimental mice were exposed to 3 defeat sessions for 2.5 min each on a single day, separated by 15 min of sensory interaction. 24 hours after the final session, mice were tested for social interaction (SI).

For evaluation of female stress responses, we utilized a vicarious defeat stress paradigm, which is a modified version of SDS to incorporate an emotional stress component to a female mouse by being allowed to witness the defeat of a male counterpart (38). In this chronic social witness defeat (CWDS), CSDS is performed as above for 10 min each session, but with a female mouse on the other side of the divider opposite the side where physical attack is taking place. Following the defeat session, the female mouse is moved to a new cage and housed on the other side of the divider opposite from a novel resident, while the male counterpart is housed opposite the resident for sensory interaction as with CSDS. During the entire CWDS, female subjects are only allowed vicarious experience without any physical interactions with male counterparts or the resident CD1s. Defeat session was repeated with a novel resident and a novel female counterpart each day for 10 consecutive days. 24 hours after the final session, female mice were tested for 3-chamber social preference test.

The CSDS, SSDS and CWDS protocols were conduct in a quiet room (<40 dB).

Behavioral tests

Social interaction test (SI)

Mice were placed in an open arena (42 x 42 cm, white walls, and floor) containing a perforated acrylic box (interaction box) centered on one wall. SI was tested first without a social target for 2.5 min, and then for another 2.5 min immediately after with a novel CD1 mouse serving as a social target. Time spent in the interaction zone (virtual area of 9 cm surrounding the interaction box) and the avoidance zone (corners

of 9 cm opposite from the interaction zone) was measured using a video tracking software (TopScan Lite 2.0, CleverSys, Reston, VA, USA).

3-Chamber Social Preference Test

Mice were placed in a rectangular arena (60 x 40 cm, white walls and floor) divided into 3 chambers (20 x 40 cm) by perforated clear acrylic dividers. The two outer chambers contain wire mesh cups, while the central chamber is empty. The experimental mouse is first placed in the central chamber of the arena with two empty wire mesh cups and allowed to explore for 5 min. Then the experimental mouse is allowed to explore the arena for an additional 5 min, this time with unfamiliar sex- and age-matched mouse in one of the wire mesh cups. The amount of time spent in the chamber containing the cups (empty or novel mouse) is measured using a video tracking software (TopScan Lite).

Forced swim test (FST)

Mice were placed in a glass cylinder (20 cm diameter) ¾ filled with water at 25±1 °C and recorded for 6 min. Time spent immobile was scored by a blinded experimenter using the software X-Plo-Rat 2005 (developed by the research team of Dr. Morato, FCLRP, USP, Brazil).

Splash test (ST)

Mice were placed in an empty glass cylinder (20 cm diameter) and had their dorsal coat sprayed three times with a viscous sucrose solution (10% sucrose v/v).

Behavior was recorded for 5 min to the evaluation of time spent grooming by a blinded experimenter using the software X-Plo-Rat 2005.

Elevated plus maze (EPM)

The EPM apparatus is a plus-shaped acrylic apparatus, elevated 50 cm above floor level with two open arms (30 cm length x 5 cm width) and two opaque closed arms (30 cm length x 5 cm width x 15 cm height) connected by a common central platform (5 cm length x 5 cm width). Mice were placed in the center of the apparatus, facing an open arm, and their behavior was recorded over 5 min to the evaluation of spatiotemporal measures, i.e., number of entries (arm entry = four paws in the arm) into the closed arms, percentage of entries into the open arms, percentage of time spent in the open arms and risk assessment behaviors, i.e., frequency of head dips and stretch attend posture (39). Behavioral analyses were performed by a blinded experimenter using the software X-Plo-Rat 2005.

Open field (OF)

To evaluate the locomotor activity and anxiety-like behavior, mice were put in the same open arena used for SI (missing the interaction box), virtually divided into a peripheric and a central zone (center square, 15 x 15 cm), for 5 min for the time spent and the distance traveled in each zone. Behavioral analyses were performed using TopScan Lite.

Sucrose preference test (SPT)

This protocol lasted for 3 days and was performed as follows: on the first day, mice were given two conical 50 mL tubes with sipper tops containing water for 24 hours. The next day, bottles were substituted with one filled with a 1% sucrose solution and one with water for 48 hours. Bottles were rotated daily to account for side preference. Sucrose preference (amount of sucrose solution consumed over water) was determined by weighing the tubes right before offering to the animals and after the end of the experiment. Solution lost by leakage or evaporation was determined by a tube placed in an empty box at the same time as the solution was offered to the animals.

Immunohistochemistry

Animals were deeply anesthetized with isoflurane and transcardially perfused with 0.1 M phosphate-buffered saline (PBS) followed by 4% paraformaldehyde (PFA). Brains were removed, post-fixed in PFA for 24 h, and 40 µm sections were collected in PBS using a vibratome (Leica VT1000S, Leica Biosystems Inc., Buffalo Grove, IL, USA). Slices were washed with PBS and blocked in 3% normal donkey serum (NDS) and 0.3% Triton X-100 in PBS for 30 min. After that, slices were incubated in a blocking buffer containing the primary antibodies rabbit anti-mCherry (1:1500; cat. No. 632496, Takara Bio USA, Inc., Mountain View, CA, USA) and chicken anti-GFP (1:1500; #GFP-1020, Aves Labs Inc., Tigard, OR, USA) at 4 °C overnight. Slices were washed again then incubated in PBS containing the secondary antibodies donkey anti-chicken Alexa 488 (1:1000; cat. No. 703-545-155, Jackson ImmunoResearch Laboratories Inc., West Grove, PA, USA) and donkey anti-rabbit Cy3 (1:1000; cat. No. 711-165-152, Jackson Immuno) at room temperature for 2 hours. Slices were washed then mounted with

Vectashield mounting media with DAPI (Vector Laboratories, Inc., Burlingame, CA, USA). Images were captured at 20x magnification on a laser-scanning confocal microscope (Leica SP8, Leica Microsystems, Buffalo Grove, IL, USA).

Cell-type-specific RNA sequencing

Immunoprecipitated polyribosomes were prepared from the VP of Npas1-Cre-RT and RT mice according to our previous protocol (40,41). RT mice were injected with AAV5-Cre virus into the VP to allow for polyribosome immunoprecipitation. VP punches were collected and pooled from 5 animals. Then the samples were homogenized and 800 μL of the supernatant was incubated in HA-coupled magnetic beads (Invitrogen: 100.03D) overnight at 4 °C. Then the magnetic beads were washed in high salt buffer and RNA was extracted with the RNeasy Micro kit (Qiagen: 74004). For RNA sequencing, samples were checked for RNA quality and only the ones with RNA integrity number > 8 were used. Samples were submitted in biological triplicates for RNA sequencing at the UMSOM Institute for Genome Sciences (IGS) and processed as described previously (41). Libraries were prepared from 10 ng of RNA from each sample using the NEBNext Ultra kit (New England BioLabs, Ipswich, MA, USA). Samples were sequenced on an Illumina HiSeq 4000 with a 75 bp paired-end read. Total of 75–110 million reads were obtained for each sample. Reads were aligned to the mouse genome using TopHat (42) and then the number of reads that aligned to the predicted coding regions was determined using HTSeq (43). Significant differential expression was assessed using Limma where genes with the absolute value of log fold change (LFC) ≥ 1 and an uncorrected p-value<0.05 in the pairwise comparisons were

considered as differentially expressed (Supplemental Data 1). Transcriptional regulator network was obtained with iRegulon app (44) using Cytoscape 3.7.2 software (45), and Gene Ontology functional enrichment analysis using PANTHER Classification System website (46) and BiNGO app (47) on Cytoscape software (Supplemental Data 2). Top GO terms were selected based off of highest $-\log_{10}$(adjusted-p-value), and Top upstream regulators were selected from the iRegulon generated list if it contained the highest number of predicted of DEGs. To validate enrichment of the NPAS1 gene, we synthetized cDNA using immunoprecipitated samples from Npas1-Cre-RT and RT mice (see above for detailed procedure) using the iScript cDNA synthesis kit (Bio-Rad). cDNA was preamplified using TaqMan Gene Expression Assay system (Applied Biosystems) as previously described (48). FAM probe for *npas1* and gadph (20× TaqMan Gene Expression Assay, Applied Biosystems) was used to amplify the products, and then qRT-PCR was run with TaqMan Gene expression Master Mix (2×, Applied Biosystems) on a CFX-384 Touch (Bio-Rad). Quantification of mRNA changes was performed using the ΔΔCT method (49).

Statistical analyses

Data were expressed as mean±s.e.m and statistical analysis was performed using Statistica 7 (StatSoft Inc., Tulsa, OK, USA) and GraphPad Prism 6. Depending on the experiment, data were analyzed by two-way ANOVA considering the factors virus (eYFP or DREADDs) and defeat (control or defeat), by the repeated-measures ANOVA considering the repeated factor session (no target or target) or by the Student's t-test. The test used is identified in the results section for each experiment. In cases where

ANOVA showed significant differences ($p \leq 0.05$), the Newman-Keuls *post-hoc* test was performed. Samples were excluded if animals had an inappropriate viral placement or if they failed Grubbs' outlier test. Sample sizes were determined from previous studies (33,34).

Results

Ventral pallidum Npas1+ neuron chemogenetic activation during subthreshold social defeat stress

For neuronal activation during SSDS, Npas1-Cre male mice received the excitatory DREADD hM3Dq into the VP and, 30 min before the SSDS, received 1 mg/kg of CNO *i.p*. On the following days, social interaction (SI) was measured followed by the forced swim test (FST) (Figure 1A), the latter a common behavior to test antidepressant action.

Chemogenetic activation of VP Npas1+ neurons induced social avoidance in SSDS mice compared to non-stressed mice. Repeated measures ANOVA revealed a significant effect of stress ($F_{1,30}$=4.42, $p<0.05$), interaction between virus and stress ($F_{1,30}$=10.68, $p<0.01$), and an interaction between virus, stress and SI session ($F_{1,30}$=4.25, $p<0.05$) for time spent in the interaction zone (Figure 1B). Using *post hoc* comparisons, the hM3Dq-SSDS group showed a decrease in the time spent in the interaction zone when target was present compared to the eYFP-Control, eYFP-SSDS, and hM3Dq-Control. Repeated measures ANOVA revealed a significant effect of the interaction between virus and stress ($F_{1,30}$=9.66, $p<0.01$), the SI session ($F_{1,30}$=10.20, $p<0.01$) and the interaction between virus, stress, and SI session ($F_{1,30}$=6.33, $p<0.05$) for the time spent in the avoidance zone (Figure 1C). The hM3Dq-SSDS group showed an increase in time spent in the avoidance zone when target was present compared to eYFP-Control, eYFP-SSDS, hM3Dq-Control, and compared to itself when the target was absent.

In the FST, chemogenetic activation of VP Npas1+ neurons induced an increase in time immobile in SSDS animals. The two-way ANOVA revealed a significant effect for virus ($F_{1,30}$=5.08, $p<0.05$) and stress ($F_{1,30}$=17.41, $p<0.001$) in time spent immobile during the FST (Figure 1D). The *post hoc* test showed an increase in time spent immobile in the hM3Dq-SSDS group compared to eYFP-Control, eYFP-SSDS, and hM3Dq-Control.

Ventral pallidum Npas1+ neuron chemogenetic inhibition during subthreshold social defeat stress

For neuronal inhibition, Npas1-Cre male mice received the inhibitory DREADD hM4Di into the VP and, 30 min before the SSDS, received 1 mg/kg of CNO *i.p*. Behaviors were assessed in the same sequence as the activation group (Figure 1A).

The inhibition of the VP Npas1+ neurons did not alter the behavioral response to the SSDS in both the SI and FST. The repeated-measures ANOVA showed a significant effect of the SI session ($F_{1,26}$=12.91, $p<0.001$) for time spent in the interaction zone (Figure 1E), indicating an increase in the time spent in the interaction zone when the target was present in all groups. No significant alterations were found for time spent in the avoidance zone ($p>0.1$) (Figure 1F) and for time spent immobile during the FST (Figure 1G).

Ventral pallidum Npas1+ neuron chemogenetic inhibition during chronic social defeat stress

For chemogenetic inhibition of VP Npas1+ neurons during CSDS, Npas1-Cre male mice received the inhibitory DREADD hM4Di into the VP and received 1 mg/kg of CNO *i.p*. 30 min before each defeat session during 10 days of CSDS. On the day after the final defeat session of CSDS, SI was performed followed by FST 24 hours later (Figure 2A).

VP Npas1+ neurons chemogenetic inhibition blocked stress-induced social avoidance in CSDS mice. Repeated-measures ANOVA showed a significant effect of the interaction between virus and SI session ($F_{1,23}$=4.85, $p<0.05$), stress and SI session ($F_{1,23}$=10.89, $p < 0.01$) and virus, stress, and SI session ($F_{1,23}$=4.22, $p=0.05$) for the time spent in the interaction zone (Figure 2B). The eYFP-CSDS group spent less time in the interaction zone when the target was present when compared to the eYFP-Control, hM4Di-Control, hM4Di-CSDS, and, compared to itself when the target was absent. No significant alterations were found for time spent in the avoidance zone ($p>0.1$) (Figure 2C).

Chemogenetic inhibition of VP Npas1+ neurons reduced time immobile in the FST after CSDS (Figure 2D). Two-way ANOVA showed a significant effect for stress ($F_{1,23}$=33.26, $p<0.001$) and interaction between virus and stress ($F_{1,23}$=6.65, $p<0.05$). The eYFP-CSDS group spent more time immobile when compared to the eYFP-Control, hM4Di-Control, and hM4Di-CSDS groups, while the hM4Di-CSDS group spent more time immobile compared to the eYFP-Control and hM4Di-Control groups.

Ventral pallidum Npas1+ neuron chemogenetic activation during behavioral tests related to anxiety and motivation

To characterize baseline behavioral effects of VP Npas1+ neuron activation, Npas1-Cre male mice received the excitatory DREADD hM3Dq into the VP and 30 min before each behavioral test, received 1 mg/kg of CNO *i.p* (Figure 3A).

In the EPM, the number of closed arm entries was not affected by the chemogenetic activation (t_{16}=0.35, p>0.5) (Figure 3B), as well as the percentage of entries (t_{16}=1.29, p>0.1) (Figure 3C, left) and time (t_{16}=0.77, p>0.1) (Figure 3C, right) in the open arms. However, activation of the VP Npas1+ neurons increased the frequency of stretch attend postures (t_{16}=2.31, p<0.05) (Figure 3D, left), decreased the frequency of head dips (t_{16}=2.29, p<0.05) (Figure 3D, right) and increased the percentage of protected stretch attend postures (t_{16}=2.08, p=0.05) (Figure 3E) in the EPM.

In the OF, chemogenetic activation of VP Npas1+ decreased the distance travelled in the center (t_{16}=2.24, p<0.05) (Figure 3F, left) but not the total distance travelled (t_{16}=1.61, p>0.1) (Figure 3F, right) nor the time spent in the center (t_{16}=0.67, p>0.5) (Figure 3G).

Social interaction was not affected by VP Npas1+ neuron activation, similar to non-stressed animals in Figure 1. There was a significant effect of SI session for the time spent in the interaction zone ($F_{1,16}$=15.78, p<0.01) (Figure 3H) and for the time spent in the corners ($F_{1,16}$=6.99, p<0.01) (Figure 3I), indicating an increase in time spent in the interaction zone when the target was present in all groups.

There was no significant alteration in time spent grooming in the ST (t_{16}=0.97, p>0.1) (Figure 3J), sucrose preference (t_{16}=0.13, p>0.5) (Figure 3K) or sucrose consumption in the SPT (t_{16}=0.43, p>0.5) (Figure 3L).

Ventral pallidum Npas1+ neuron chemogenetic inhibition during the chronic witness defeat stress in females

To examine the effects of chemogenetic inhibition of VP Npas1+ neurons during chronic social stress in females, female Npas1-Cre mice received the inhibitory DREADD hM4Di into the VP and received 1 mg/kg of CNO *i.p*. 30 min before each witness defeat session during 10 days of CWDS. On the day after the final defeat session of CSDS, social preference was tested in the 3-chamber social preference test (Figure 4A).

In this test, female mice that did not receive inhibitory DREADD (eYFP) reduced their social interaction after they underwent CWDS (Figure 4B). However, mice that received inhibitory DREADD hM4Di into the VP were not affected by CWDS and showed similar levels of social preference compared to the non-stressed control mice. All the groups except for the eYFP-CWDS group increased their interaction when the target animals were present (Figure 4B). The repeated-measures ANOVA showed a significant effect of the session ($F_{1,27}$=21.77, p<0.0001) but no significant effects of virus treatment or interaction ($F_{3,27}$=2.76 p=0.061 and $F_{3,27}$=0.71, p=0.55, respectively). *Post hoc* test showed significantly increased interaction time with the target present in all groups except for the eYFP-CWDS group.

Viral tracing of ventral pallidum Npas1+ neuron projection targets

Using a DIO-eYFP in Npas1-Cre mice, which contains TdTomato fluorophores within Npas1+ cells, the projection targets of VP Npas1+ neurons were characterized. After confirming the injection site in the VP (Figure 5), we were able to identify eYFP-

positive neuronal fibers within the NAc, VTA, medial and lateral habenula, lateral hypothalamus, mediodorsal, paraventricular and centrolateral thalamic nuclei, medial and lateral septum, and periaqueductal gray area (Figure 5). We also identified eYFP-positive neuronal fiber within the medial anterior olfactory nucleus (AOM) and lateral anterior olfactory nucleus (AOL) (Supplemental Data 3) Among these regions, fibers were found to be close to Npas1+ neurons within the NAc, the lateral hypothalamus, anterior olfactory nucleus, and the lateral septum. Other regions did not contain many Npas1+ cells.

Genetic profiling of ventral pallidum Npas1+ neurons

Using Npas1-Cre-RT mice, we isolated ribosome-associated mRNA from VP Npas1+ neurons, which was analyzed for their genetic profile relative to all VP neurons. This approach is cell-type specific (50), and allowed us to specific analyze the genetic profile of the Npas1+ neurons. mRNA used for sequencing was used for validation of Npas1 gene enrichment, as it was confirmed that there was a 4.98-fold enrichment (Figure 6A, $t_8 = 7.881$, $p < 0.0001$). Out of 23,843 total genes analyzed, 2,297 genes were identified as differentially expressed (DEGs, Figure 6B), of which 562 genes were identified as significantly enriched in Npas1+ neurons compared to nonspecific VP neurons. Top entries from Biological Process GO term analysis based on p-value were nervous system development and neurogenesis, and the top terms from Molecular Function section were protein binding, cytoskeletal protein binding, and chloride channel activity (Figure 6C). To further investigate whether these enriched genes are regulated by a common transcription factor in Npas1+ neurons within the VP, upstream regulator

prediction analysis was performed. Transcription factors SOX6 and SMAD2 had the highest number of predicted DEG targets (Figure 6D). Several SOX6 and SMAD2 targets, including *Sema6a* and *Sox6* were associated with the Top GO terms, Neurogenesis and Development of Nervous System.

Discussion

Here we show that the chemogenetic activation of VP Npas1+ neurons increased the susceptibility to SDS in male mice, while the inactivation of these neurons increased resilience to chronic social stress in both male and female mice. The activation of VP Npas1+ neurons also increased anxiety-like behaviors evaluated in the EPM and OF. Moreover, we found that these neurons have diverse projection targets, which we highlight the NAc, LHb, and VTA.

Overall, the behavioral consequences of manipulating the VP activity are diverse. Some results showed that inhibiting the whole VP by increasing GABAergic tonic inhibition in this region increases depressive-like behaviors (51), while activating orexinergic receptors in GABAergic VP neurons is antidepressant (52). On the other hand, silencing specifically the VP PV+ neurons decreases depressive-like behaviors (10), as well as the inhibition of glutamatergic neurons projecting to the LHb exerts antidepressant-like effects (53). In our work, the activation of the VP Npas1+ neurons increases susceptibility to a sub-threshold social stressor, whereas their inhibition decreased depressive-like behaviors after repeated social stress. Together, such results suggest that different neuronal types within the VP differentially control behavioral responses to stress, similar to other brain regions, such as the NAc (2). These findings increment the knowledge of VP neurons subtype role in behavioral response to aversive and rewarding stimuli (5).

There was an increase in anxiety-like behaviors in the EPM and the OF due to the activation of the VP Npas1+ neurons in our study. This increase in anxiety-like behaviors is in line with increased susceptibility to stress in these same conditions. In

humans, an anxious temperament or anxiety during young life is correlated to increased risk for depression in adulthood (54), and the prevalence of anxiety and depression is increased in individuals with a negative coping style to stress (55,56). Similar to its role in the behavioral responses to stress, different VP neuronal types seem to have opposite effects on anxiety-like behaviors. Increasing the activity of the whole VP with bicuculine (a $GABA_A$ receptor antagonist) is anxiolytic (57), as well as the activation of the VP GABAergic neurons (58). Both neurotensin and substance P, when administered in the VP, decrease anxiety-like behaviors (59,60), together with an increase in VP activity (61,62).

No studies exist regarding the electrophysiological proprieties and connections of the VP Npas1+ neurons. However, the similarities between the GP and the VP could help to understand the cellular proprieties of the VP Npas1+ neurons. Both regions are originated from similar progenitors and are comprised of similar neuron classes (4,63,64). Both the VP and the GP are comprised of glutamatergic, cholinergic, and GABAergic neurons, the latter comprising the majority of VP neurons. In the GP, GABAergic neurons could be classified into three subgroups, highly segregated according to their electrical properties and the expression of genetic markers (29). Among these markers, the Npas1 and PV markers differentiate two projection patterns. The Npas1+ neurons constitute the principal projection to the dorsal striatum while the PV+ neurons project mainly to the subthalamic nucleus (27,30). There are also projections of the Npas1+ neurons to the somatosensory, somatomotor, and orbital cortex (28). Our results revealed that, compared to the GP, Npas1+ neurons in the VP have a more ventral pattern of projection, without projecting to cortical areas. Others

have found similar neuronal projections when looking to the VP as a whole (4,5,8,10). It suggests that these neurons in the VP should be more involved in regulating emotional processing instead of a prominent role in motor processing.

Among the brain targets of VP Npas1+ neurons found in our study, the NAc, the VTA, and the LHb have been recently implicated in the development of depression (3,9). Since most evidence suggests that Npas1+ neurons are GABAergic, at least in the GP (27,29,30), we can propose hypotheses at the circuitry level.

The first hypothesis is that the Npas1+ neurons mediate susceptibility to SDS through their activation and release of GABA within the NAc, increasing the inhibition of the D1-MSNs compared to D2-MSNs. Chemogenetic inhibition of the D1-MSNs increases susceptibility to the SDS, while inhibition of the D2-MSNs does not affect SDS behavior (65). Contrary to this hypothesis, VP equally projects to both D1 and D2-MSNs (66,67) and the D2-MSNs are more sensitive to GABA-induced hyperpolarization (30,68). Furthermore, recent results have shown that arkypallidal VP neurons (which resembles arkypallidal neurons within the GP that are Npas1+) projects to the NAc, releasing GABA onto MSNs and promoting reward consumption (69).

VP projections to the LHb are both excitatory and inhibitory (5). Evidence shows that optogenetic activation of glutamatergic VP neurons induces place aversion (23), and increases behavioral despair in response to SDS (10). Considering the possibility that VP Npas1+ neurons release glutamate within the LHb, another hypothesis is that chemogenetic activation of VP neurons is inducing susceptibility to SDS through increasing LHb activity. Future studies are needed to determine if Npas1+ neurons in VP primarily release GABA, similar to these neurons in the GP (27,29,30).

VTA activity is altered in subjects susceptible to the SDS (70–72). Following stress, these individuals have increased VTA dopaminergic neuron firing, specifically to the NAc (71). VP activity to VTA is also altered after stress exposure. VP projections to VTA are both glutamatergic and GABAergic and target both dopaminergic and GABAergic interneurons in the VTA, respectively. Increased activity of VP projecting neurons to VTA increase the activity of dopaminergic VTA neurons and increase the susceptibility to SDS (10). From these results, we can deduce another possibility in which the VP Npas1+ projections to the VTA increase the activity of dopaminergic neurons through the GABAergic interneurons, and thus increasing susceptibility to SDS.

We also have analyzed cell-type specific transcriptome of Npas1+ neurons within the VP. We have identified enriched genes, biological processes and transcription factors that may point to potential novel function of Npas1+ neurons distinct from Npas1- VP neurons. Sox6 being a specific transcriptional factor is particularly interesting, as a recent anatomical study using Sox6-Cre mouse suggests that Sox6+ neurons are a distinct type of neurons within the GP (28). Furthermore, it is also revealed in this study that about 93% of Npas1+ neurons within the GP are Sox6+, suggesting a possible functional relationship between these TFs. Whether such anatomical description is true for VP Npas1+ neurons remain unknown. Cell-type specific transcriptome also revealed that VP Npas1+ neurons differentially express some genes related to glutamate synthesis and release, while the expression of genes related to GABA neurotransmission seems to be not upregulated. In this context, we highlight the expression of slc17a6 gene, which encodes the transcription of the vesicular glutamate transporter 2 (VGLUT2) (73,74) and the slc38a2 gene, which

encodes the sodium-coupled amino acid transporter 2 (SNAT2) (75). We also found a differential expression of slc44a1 and th genes (Supplemental Data 1).

In conclusion, the activity of Npas1+ neurons in the VP modulates the susceptibility to SDS. Their activity could be related to their projections to brain regions that modulate rewarding and aversion, such as the NAc, the LHb, and the VTA. Future studies can elucidate the VP Npas1+ neuron circuitry responsible for these stress outcomes.

Acknowledgments and Disclosures

This work was supported by NIH R01MH106500 and R01DA047843 to MKL, R01NS069777 and R01MH112768 to CSC, grants no. 2015/25308-3 and 2018/05496-8 from São Paulo Research Foundation (FAPESP) to GM-S and financed in part by the Coordenação de Aperfeiçoamento de Pessoal de Nível Superior - Brasil (CAPES) - Finance Code 001. FAPESP and CAPES had no further role in the study design; in the collection, analysis, or interpretation of data; in the writing of the report; or in the decision to submit the paper for publication.

The authors report no biomedical financial interests or potential conflicts of interest.

References

1. Russo SJ, Nestler EJ (2013): The brain reward circuitry in mood disorders. *Nat Rev Neurosci* 14: 609–625.

2. Francis TC, Lobo MK (2017): Emerging Role for Nucleus Accumbens Medium Spiny Neuron Subtypes in Depression. *Biol Psychiatry* 81: 645–653.

3. Fox ME, Lobo MK (2019): The molecular and cellular mechanisms of depression: a focus on reward circuitry. *Mol Psychiatry*. https://doi.org/10.1038/s41380-019-0415-3

4. Root DH, Melendez RI, Zaborszky L, Napier TC (2015): The ventral pallidum: Subregion-specific functional anatomy and roles in motivated behaviors. *Prog Neurobiol* 130: 29–70.

5. Wulff AB, Tooley J, Marconi LJ, Creed MC (2019): Ventral pallidal modulation of aversion processing. *Brain Res* 1713: 62–69.

6. Smith KS, Tindell AJ, Aldridge JW, Berridge KC (2009): Ventral pallidum roles in reward and motivation. *Behav Brain Res* 196: 155–167.

7. Khan HA, Urstadt KR, Mostovoi NA, Berridge KC (2020): Mapping excessive “disgust” in the brain: Ventral pallidum inactivation recruits distributed circuitry to make sweetness “disgusting.” *Cogn Affect Behav Neurosci* 20: 141–159.

8. Faget L, Zell V, Souter E, McPherson A, Ressler R, Gutierrez-Reed N, *et al.* (2018): Opponent control of behavioral reinforcement by inhibitory and excitatory projections from the ventral pallidum. *Nat Commun* 9: 849.

9. Knowland D, Lim BK (2018): Circuit-based frameworks of depressive behaviors: The

role of reward circuitry and beyond. *Pharmacol Biochem Behav* 174: 42–52.

10. Knowland D, Lilascharoen V, Pacia CP, Shin S, Wang EHJ, Lim BK (2017): Distinct Ventral Pallidal Neural Populations Mediate Separate Symptoms of Depression. *Cell* 170: 284-297.e18.

11. Stuke H, Hanken K, Hirsch J, Klein J, Wittig F, Kastrup A, Hildebrandt H (2016): Cross-Sectional and Longitudinal Relationships between Depressive Symptoms and Brain Atrophy in MS Patients. *Front Hum Neurosci* 10: 1–8.

12. Onyewuenyi IC, Muldoon MF, Christie IC, Erickson KI, Gianaros PJ (2014): Basal ganglia morphology links the metabolic syndrome and depressive symptoms. *Physiol Behav* 123: 214–222.

13. Miller JM, Vorel SR, Tranguch AJ, Kenny ET, Mazzoni P, van Gorp WG, Kleber HD (2006): Anhedonia After a Selective Bilateral Lesion of the Globus Pallidus. *Am J Psychiatry* 163: 786–788.

14. Moussawi K, Kalivas PW, Lee JW (2016): Abstinence From Drug Dependence After Bilateral Globus Pallidus Hypoxic-Ischemic Injury. *Biol Psychiatry* 80: e79–e80.

15. Murrough JW, Henry S, Hu J, Gallezot J-D, Planeta-Wilson B, Neumaier JF, Neumeister A (2011): Reduced ventral striatal/ventral pallidal serotonin1B receptor binding potential in major depressive disorder. *Psychopharmacology (Berl)* 213: 547–553.

16. Kupchik YM, Brown RM, Heinsbroek JA, Lobo MK, Schwartz DJ, Kalivas PW (2015): Coding the direct/indirect pathways by D1 and D2 receptors is not valid for accumbens projections. *Nat Neurosci* 18: 1230–1232.

17. Churchill L, Kalivas PW (1994): A topographically organized gamma-aminobutyric

acid projection from the ventral pallidum to the nucleus accumbens in the rat. *J Comp Neurol* 345: 579–595.

18. Kuo H, Chang HT (1992): Ventral pallido-striatal pathway in the rat brain: A light and electron microscopic study. *J Comp Neurol* 321: 626–636.

19. Klitenick MA, Deutch AY, Churchill L, Kalivas PW (1992): Topography and functional role of dopaminergic projections from the ventral mesencephalic tegmentum to the ventral pallidum. *Neuroscience* 50: 371–386.

20. Stout KA, Dunn AR, Lohr KM, Alter SP, Cliburn RA, Guillot TS, Miller GW (2016): Selective Enhancement of Dopamine Release in the Ventral Pallidum of Methamphetamine-Sensitized Mice. *ACS Chem Neurosci* 7: 1364–1373.

21. Taylor SR, Badurek S, Dileone RJ, Nashmi R, Minichiello L, Picciotto MR (2014): GABAergic and glutamatergic efferents of the mouse ventral tegmental area. *J Comp Neurol* 522: 3308–3334.

22. Breton JM, Charbit AR, Snyder BJ, Fong PTK, Dias E V., Himmels P, *et al.* (2019): Relative contributions and mapping of ventral tegmental area dopamine and GABA neurons by projection target in the rat. *J Comp Neurol* 527: 916–941.

23. Tooley J, Marconi L, Alipio JB, Matikainen-Ankney B, Georgiou P, Kravitz A V., Creed MC (2018): Glutamatergic Ventral Pallidal Neurons Modulate Activity of the Habenula–Tegmental Circuitry and Constrain Reward Seeking. *Biol Psychiatry* 83: 1012–1023.

24. Tripathi A, Prensa L, Mengual E (2013): Axonal branching patterns of ventral pallidal neurons in the rat. *Brain Struct Funct* 218: 1133–1157.

25. Stanco A, Pla R, Vogt D, Chen Y, Mandal S, Walker J, *et al.* (2014): NPAS1

Represses the Generation of Specific Subtypes of Cortical Interneurons. *Neuron* 84: 940–953.

26. Teh CHL, Lam KKY, Loh CC, Loo JM, Yan T, Lim TM (2006): Neuronal PAS Domain Protein 1 Is a Transcriptional Repressor and Requires Arylhydrocarbon Nuclear Translocator for Its Nuclear Localization. *J Biol Chem* 281: 34617–34629.
27. Hernandez VM, Hegeman DJ, Cui Q, Kelver DA, Fiske MP, Glajch KE, *et al.* (2015): Parvalbumin+ Neurons and Npas1+ Neurons Are Distinct Neuron Classes in the Mouse External Globus Pallidus. *J Neurosci* 35: 11830–11847.
28. Abecassis ZA, Berceau BL, Win PH, García D, Xenias HS, Cui Q, *et al.* (2020): Npas1 + -Nkx2.1 + Neurons Are an Integral Part of the Cortico-pallido-cortical Loop. *J Neurosci* 40: 743–768.
29. Abrahao KP, Lovinger DM (2018): Classification of GABAergic neuron subtypes from the globus pallidus using wild-type and transgenic mice. *J Physiol* 596: 4219–4235.
30. Glajch KE, Kelver DA, Hegeman DJ, Cui Q, Xenias HS, Augustine EC, *et al.* (2016): Npas1+ Pallidal Neurons Target Striatal Projection Neurons. *J Neurosci* 36: 5472–5488.
31. Hunt AJ, Dasgupta R, Rajamanickam S, Jiang Z, Beierlein M, Chan CS, Justice NJ (2018): Paraventricular hypothalamic and amygdalar CRF neurons synapse in the external globus pallidus. *Brain Struct Funct* 223: 2685–2698.
32. Sanz E, Yang L, Su T, Morris DR, McKnight GS, Amieux PS (2009): Cell-type-specific isolation of ribosome-associated mRNA from complex tissues. *Proc Natl Acad Sci U S A* 106: 13939–13944.

33. Nam H, Chandra R, Francis TC, Dias C, Cheer JF, Lobo MK (2019): Reduced nucleus accumbens enkephalins underlie vulnerability to social defeat stress. *Neuropsychopharmacology* 44: 1876–1885.

34. Fox ME, Chandra R, Menken MS, Larkin EJ, Nam H, Engeln M, *et al.* (2020): Dendritic remodeling of D1 neurons by RhoA/Rho-kinase mediates depression-like behavior. *Mol Psychiatry* 25: 1022–1034.

35. Chandra R, Francis TC, Nam H, Riggs LM, Engeln M, Rudzinskas S, *et al.* (2017): Reduced Slc6a15 in Nucleus Accumbens D2-Neurons Underlies Stress Susceptibility. *J Neurosci* 37: 6527–6538.

36. Fox ME, Figueiredo A, Menken MS, Lobo MK (2020): Dendritic spine density is increased on nucleus accumbens D2 neurons after chronic social defeat. *Sci Rep* 10: 12393.

37. Golden SA, Covington HE, Berton O, Russo SJ (2011): A standardized protocol for repeated social defeat stress in mice. *Nat Protoc* 6: 1183–1191.

38. Iñiguez SD, Flores-Ramirez FJ, Riggs LM, Alipio JB, Garcia-Carachure I, Hernandez MA, *et al.* (2018): Vicarious Social Defeat Stress Induces Depression-Related Outcomes in Female Mice. *Biol Psychiatry* 83: 9–17.

39. Morais-Silva G, Fernandes-Santos J, Moreira-Silva D, Marin MT (2016): Concomitant stress potentiates the preference for, and consumption of, ethanol induced by chronic pre-exposure to ethanol. *Brazilian J Med Biol Res* 49: 1–9.

40. Chandra R, Calarco CA, Lobo MK (2019): Differential mitochondrial morphology in ventral striatal projection neuron subtypes. *J Neurosci Res* 97: 1579–1589.

41. Engeln M, Song Y, Chandra R, La A, Fox ME, Evans B, *et al.* (2020): Individual

differences in stereotypy and neuron subtype translatome with TrkB deletion. *Mol Psychiatry*. https://doi.org/10.1038/s41380-020-0746-0

42. Kim D, Pertea G, Trapnell C, Pimentel H, Kelley R, Salzberg SL (2013): TopHat2: accurate alignment of transcriptomes in the presence of insertions, deletions and gene fusions. *Genome Biol* 14: R36.
43. Anders S, Huber W (2010): Differential expression analysis for sequence count data. *Genome Biol* 11: R106.
44. Janky R, Verfaillie A, Imrichová H, Van de Sande B, Standaert L, Christiaens V, *et al.* (2014): iRegulon: From a Gene List to a Gene Regulatory Network Using Large Motif and Track Collections ((H. J. Bussemaker, editor)). *PLoS Comput Biol* 10: e1003731.
45. Shannon P, Markiel A, Ozier O, Baliga NS, Wang JT, Ramage D, *et al.* (2003): Cytoscape: a software environment for integrated models of biomolecular interaction networks. *Genome Res* 13: 2498–504.
46. Mi H, Muruganujan A, Casagrande JT, Thomas PD (2013): Large-scale gene function analysis with the PANTHER classification system. *Nat Protoc* 8: 1551–1566.
47. Maere S, Heymans K, Kuiper M (2005): BiNGO: a Cytoscape plugin to assess overrepresentation of Gene Ontology categories in Biological Networks. *Bioinformatics* 21: 3448–3449.
48. Liu Q-R, Rubio FJ, Bossert JM, Marchant NJ, Fanous S, Hou X, *et al.* (2014): Detection of molecular alterations in methamphetamine-activated Fos-expressing neurons from a single rat dorsal striatum using fluorescence-activated cell sorting

(FACS). *J Neurochem* 128: 173–185.

49. Chandra R, Francis TC, Konkalmatt P, Amgalan A, Gancarz AM, Dietz DM, Lobo MK (2015): Opposing Role for Egr3 in Nucleus Accumbens Cell Subtypes in Cocaine Action. *J Neurosci* 35: 7927–7937.
50. Sanz E, Yang L, Su T, Morris DR, McKnight GS, Amieux PS (2009): Cell-type-specific isolation of ribosome-associated mRNA from complex tissues. *Proc Natl Acad Sci U S A* 106: 13939–13944.
51. Skirzewski M, López W, Mosquera E, Betancourt L, Catlow B, Chiurillo M, *et al.* (2011): Enhanced GABAergic tone in the ventral pallidum: Memory of unpleasant experiences? *Neuroscience* 196: 131–146.
52. Ji MJ, Zhang XY, Chen Z, Wang JJ, Zhu JN (2019): Orexin prevents depressive-like behavior by promoting stress resilience. *Mol Psychiatry* 24: 282–293.
53. Liu B, Cao Y, Wang J, Dong J (2020): Excitatory transmission from ventral pallidum to lateral habenula mediates depression. *World J Biol Psychiatry* 2975. https://doi.org/10.1080/15622975.2020.1725117
54. Kalin NH (2017): Mechanisms underlying the early risk to develop anxiety and depression: A translational approach. *Eur Neuropsychopharmacol* 27: 543–553.
55. Lew B, Huen J, Yu P, Yuan L, Wang D-F, Ping F, *et al.* (2019): Associations between depression, anxiety, stress, hopelessness, subjective well-being, coping styles and suicide in Chinese university students. *PLoS One* 14: e0217372.
56. Xiong W, Liu H, Gong P, Wang Q, Ren Z, He M, *et al.* (2019): Relationships of coping styles and sleep quality with anxiety symptoms among Chinese adolescents: A cross-sectional study. *J Affect Disord* 257: 108–115.

57. Reichard RA, Parsley KP, Subramanian S, Stevenson HS, Schwartz ZM, Sura T, Zahm DS (2019): The lateral preoptic area and ventral pallidum embolden behavior. *Brain Struct Funct* 224: 1245–1265.

58. Li Y-D, Luo Y-J, Xu W, Ge J, Cherasse Y, Wang Y-Q, *et al.* (2020): Ventral pallidal GABAergic neurons control wakefulness associated with motivation through the ventral tegmental pathway. *Mol Psychiatry*. https://doi.org/10.1038/s41380-020-00906-0

59. Ollmann T, Péczely L, László K, Kovács A, Gálosi R, Kertes E, *et al.* (2015): Anxiolytic effect of neurotensin microinjection into the ventral pallidum. *Behav Brain Res* 294: 208–214.

60. Nikolaus S, Huston JP, Hasenöhrl RU (2000): Anxiolytic-like effects in rats produced by ventral pallidal injection of both N- and C-terminal fragments of substance P. *Neurosci Lett* 283: 37–40.

61. Michaud J-C, Gueudet C, Soubrié P (2000): Effects of neurotensin receptor antagonists on the firing rate of rat ventral pallidum neurons. *Neuroreport* 11: 1437–1441.

62. Napier TC, Mitrovic I, Churchill L, Klitenick MA, Lu X-Y, Kalivas PW (1995): Substance P in the ventral pallidum: Projection from the ventral striatum, and electrophysiological and behavioral cinsequences of pallidal substance P. *Neuroscience* 69: 59–70.

63. Ma TP, Geyer HL (2018): The Basal Nuclei. *Fundamental Neuroscience for Basic and Clinical Applications*. Elsevier, pp 377-393.e1.

64. Nobrega-Pereira S, Gelman D, Bartolini G, Pla R, Pierani A, Marin O (2010): Origin

and Molecular Specification of Globus Pallidus Neurons. *J Neurosci* 30: 2824–2834.

65. Francis TC, Chandra R, Friend DM, Finkel E, Dayrit G, Miranda J, *et al.* (2015): Nucleus accumbens medium spiny neuron subtypes mediate depression-related outcomes to social defeat stress. *Biol Psychiatry* 77: 212–222.

66. Gangarossa G, Espallergues J, de Kerchove d'Exaerde A, El Mestikawy S, Gerfen CR, Hervé D, *et al.* (2013): Distribution and compartmental organization of GABAergic medium-sized spiny neurons in the mouse nucleus accumbens. *Front Neural Circuits* 7: 1–20.

67. Li Z, Chen Z, Fan G, Li A, Yuan J, Xu T (2018): Cell-Type-Specific Afferent Innervation of the Nucleus Accumbens Core and Shell. *Front Neuroanat* 12: 1–16.

68. Ade KK, Janssen MJ, Ortinski PI, Vicini S (2008): Differential Tonic GABA Conductances in Striatal Medium Spiny Neurons. *J Neurosci* 28: 1185–1197.

69. Vachez YM, Tooley JR, Abiraman K, Matikainen-Ankney B, Casey E, Earnest T, *et al.* (2021): Ventral arkypallidal neurons inhibit accumbal firing to promote reward consumption. *Nat Neurosci*. https://doi.org/10.1038/s41593-020-00772-7

70. Cao J-L, Cooper DC, Han M-H, Covington III HE, Wilkinson MB, Nestler EJ, *et al.* (2010): Mesolimbic dopamine neurons in the brain reward circuit mediate susceptibility to social defeat and antidepressant action. *J Neurosci* 30: 16453–16458.

71. Chaudhury D, Walsh JJ, Friedman AK, Juarez B, Ku SM, Koo JW, *et al.* (2013): Rapid regulation of depression-related behaviours by control of midbrain dopamine neurons. *Nature* 493: 532–536.

72. Krishnan V, Han M-H, Graham DL, Berton O, Renthal W, Russo SJ, *et al.* (2007):

Molecular Adaptations Underlying Susceptibility and Resistance to Social Defeat in Brain Reward Regions. *Cell* 131: 391–404.

73. Hayashi M, Otsuka M, Morimoto R, Hirota S, Yatsushiro S, Takeda J, *et al.* (2001): Differentiation-associated Na+-dependent Inorganic Phosphate Cotransporter (DNPI) Is a Vesicular Glutamate Transporter in Endocrine Glutamatergic Systems. *J Biol Chem* 276: 43400–43406.

74. El Mestikawy S, Wallén-Mackenzie Å, Fortin GM, Descarries L, Trudeau LE (2011): From glutamate co-release to vesicular synergy: Vesicular glutamate transporters. *Nat Rev Neurosci* 12: 204–216.

75. González-González IM, Cubelos B, Giménez C, Zafra F (2005): Immunohistochemical localization of the amino acid transporter SNAT2 in the rat brain. *Neuroscience* 130: 61–73.

Figure captions

Figure 1. Chemogenetic activation of the VP Npas1 neurons increases the susceptibility to the subthreshold social defeat stress (SSDS) in male mice. **A**, representative timeline of the experiments involving the manipulation of the VP Npas1 neurons during the SSDS. **B, C, D**, effects of the chemogenetic activation of the VP Npas1 neurons using the hM3Dq DREADDs during the SSDS in the social interaction (SI) and forced swim (FST) tests. **E**, **F, G,** effects of the chemogenetic inhibition of the VP Npas1 neurons using the hM4Di DREAADs during the SSDS in the SI and FST. Data is presented as mean + the individual values obtained for each animal (n = 5-9 animals per group). *, **, *** indicates $p < 0.05$, $p < 0.01$, $p < 0.001$, respectively.

Figure 2. Chemogenetic inhibition of the VP Npas1 neurons decreases the susceptibility to the chronic social defeat stress (CSDS) in male mice. **A**, representative

timeline of the experiments involving the inhibition of the VP Npas1 neurons during the CSDS. **B, C, D,** effects of the chemogenetic inhibition of the VP Npas1 neurons using the hM4Di DREAADs during the CSDS in the SI and FST. Data is presented as mean + the individual values obtained for each animal (n = 6-8 animals per group). *, **, *** indicates $p < 0.05$, $p < 0.01$, $p < 0.001$, respectively.

Figure 3. Chemogenetic inhibition of the VP Npas1 neurons is anxiogenic in male mice. **A**, representative timeline of the experiments involving the activation of the VP Npas1 neurons during behavioral tests that evaluate anxiety-like and depressive-like behaviors. **B, C, D, E,** effects of the chemogenetic inhibition of the VP Npas1 neurons using the hM4Di DREAADs during the elevated plus maze (EPM) test. **F, G,** effects of the chemogenetic inhibition of the VP Npas1 neurons using the hM4Di DREAADs during the open field (OF) test. **H, I,** effects of the chemogenetic inhibition of the VP Npas1 neurons using the hM4Di DREAADs during the SI. **J,** effects of the chemogenetic inhibition of the VP Npas1 neurons using the hM4Di DREAADs during the Splash test (ST). **K, L,** effects of the chemogenetic inhibition of the VP Npas1 neurons using the hM4Di DREAADs on the sucrose preference and intake on the sucrose preference test (SPT). Data is presented as mean + the individual values obtained for each animal (n = 8-9 animals per group). * indicates $p < 0.05$.

Figure 4. Chemogenetic inhibition of the VP Npas1 neurons decreases the susceptibility to the chronic witness defeat stress (CWDS) in female mice. **A**, representative timeline of the experiments involving the inhibition of the VP Npas1 neurons during the CWDS. **B,** effects of the chemogenetic inhibition of the VP Npas1 neurons using the hM4Di DREAADs during the CWDS in the 3-chamber social preference test. Data is presented as mean + the individual values obtained for each animal (n = 6-10 animals per group). *, $p < 0.05$.

Figure 5. Representative images of the DIO-eYFP expression in the brain regions that receive projection from the VP Npas1 neurons in the Npas1-cre mice. The first column (from the left) shows the expression of the eYFP (in green) within the brain regions,

while the second column shows the expression of the Npas1 marker (in red). The third column shows the merged images. The first panel is representative of a correct injection site in the ventral pallidum (VP). NAc, nucleus accumbens. Ac, anterior commissure. VTA, ventral tegmental area. Hb, habenula. LHb, lateral habenula. MHb, medial habenula. 3V, third ventricle. PVT, paraventricular nucleus of the thalamus. LH, lateral hypothalamus. Opt, optical nerve. Thal, thalamus. LS, lateral septum. PAG, periaqueductal gray matter. Aq, cerebral aqueduct.

Figure 6. Cell-type specific profiling of mRNA from VP Npas1+ neurons reveal potential functions and regulators these neurons. **A.** Validation of Npas1 enrichment in ribosome-associated mRNA from VP Npas1+ neurons used in genetic profiling. **B.** Overview of all differentially expressed genes (DEGs) identified with the distribution of log fold change (LFC) within DEGs. **C.** Top hits from Biological Process and Molecular Function GO term analysis and an example from one of the top hits, regulation of neurogenesis, with the degree of fold change of genes within the GO term. **D.** 2 Top hits from upstream regulator prediction analysis using top 2 GO terms identified, neurogenesis and development of nervous system. Predicted DEG targets of each regulator are identified with arrows along with their fold change analyzed in VP Npas1+ neurons.

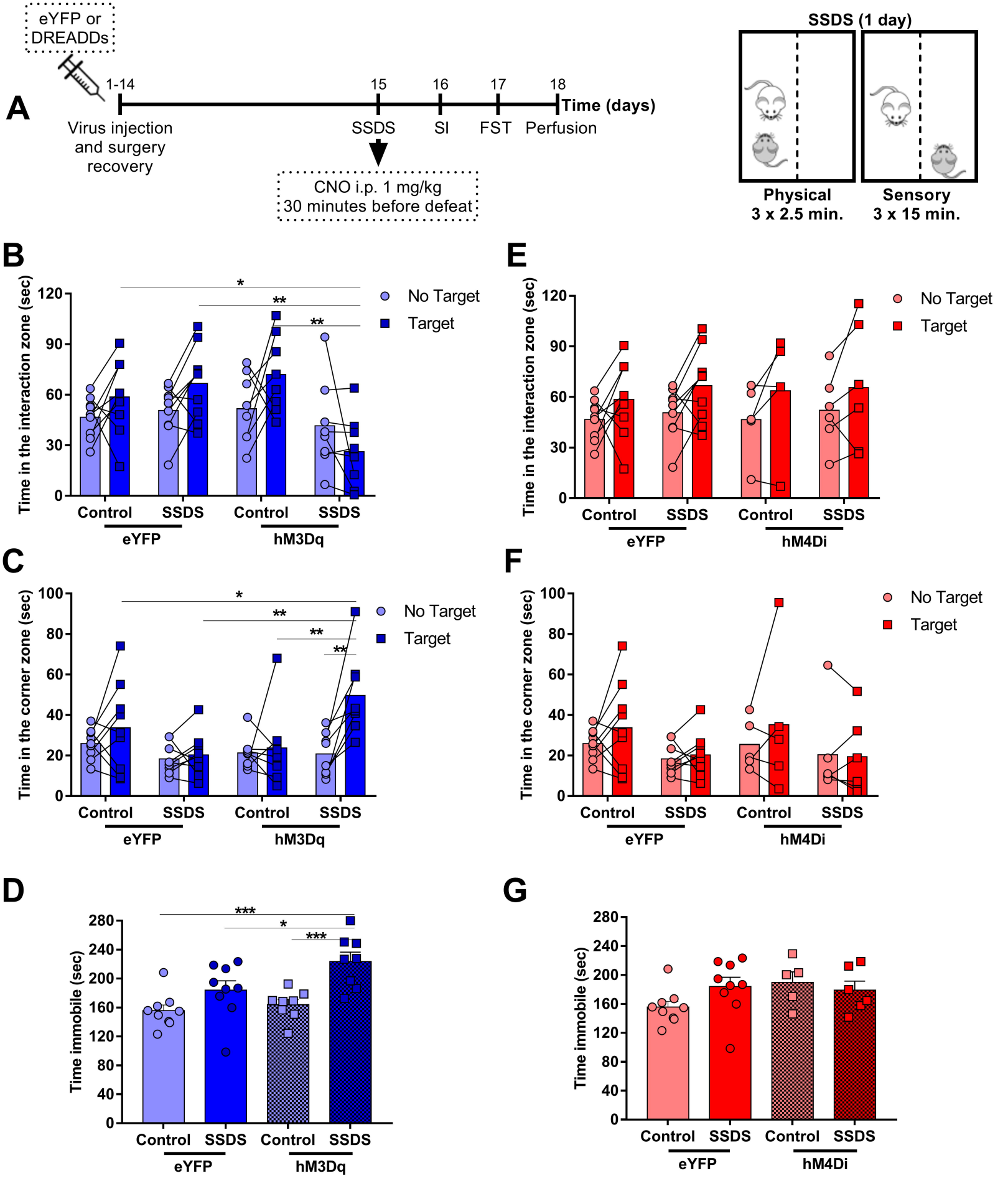
A
eYFP or DREADDs
1-14
Virus injection and surgery recovery
15
SSDS
16
SI
17
FST
18
Perfusion
Time (days)
CNO i.p. 1 mg/kg 30 minutes before defeat
SSDS (1 day)
Physical 3 x 2.5 min.
Sensory 3 x 15 min.
B
Time in the interaction zone (sec)
No Target
Target
Control
SSDS
eYFP
hM3Dq
C
Time in the corner zone (sec)
D
Time immobile (sec)
E
hM4Di
F
G

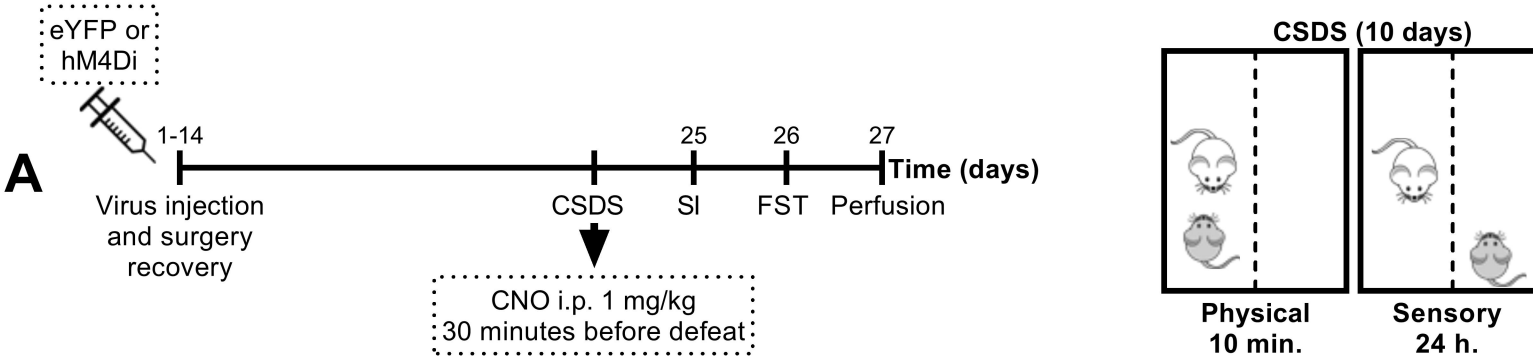
A
eYFP or hM4Di
1-14
Virus injection and surgery recovery
CSDS
25
SI
26
FST
27
Perfusion
Time (days)
CNO i.p. 1 mg/kg
30 minutes before defeat
CSDS (10 days)
Physical
10 min.
Sensory
24 h.

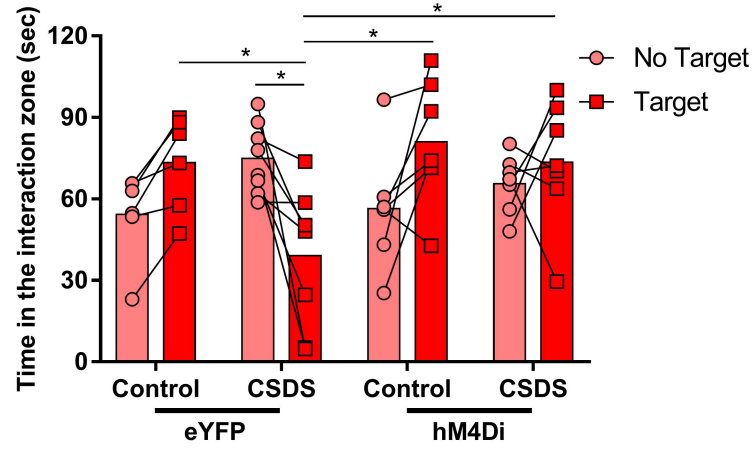
B
Time in the interaction zone (sec)
120
90
60
30
0
No Target
Target
Control
CSDS
Control
CSDS
eYFP
hM4Di

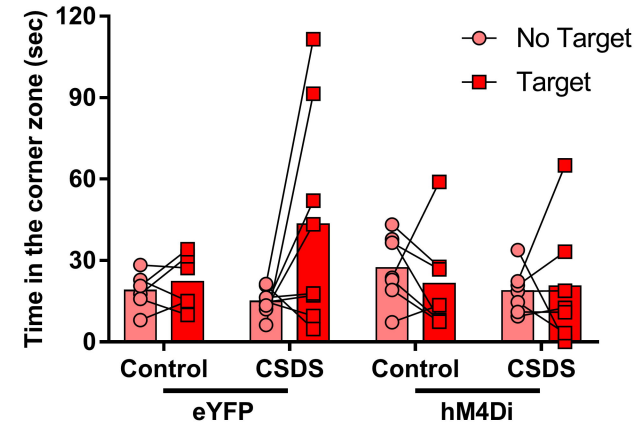
C
Time in the corner zone (sec)
120
90
60
30
0
No Target
Target
Control
CSDS
Control
CSDS
eYFP
hM4Di

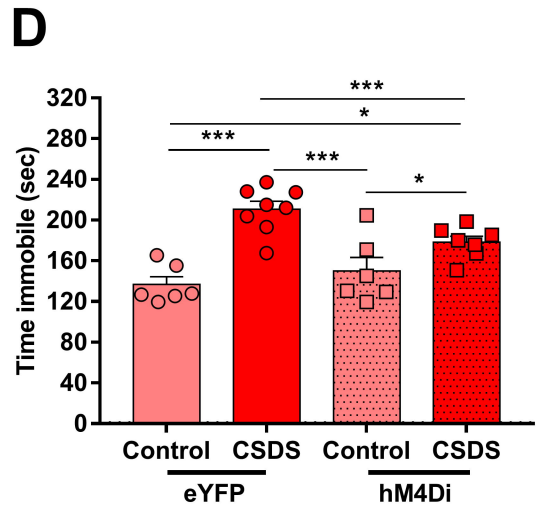
D
Time immobile (sec)
320
280
240
200
160
120
80
40
0
Control
CSDS
Control
CSDS
eYFP
hM4Di

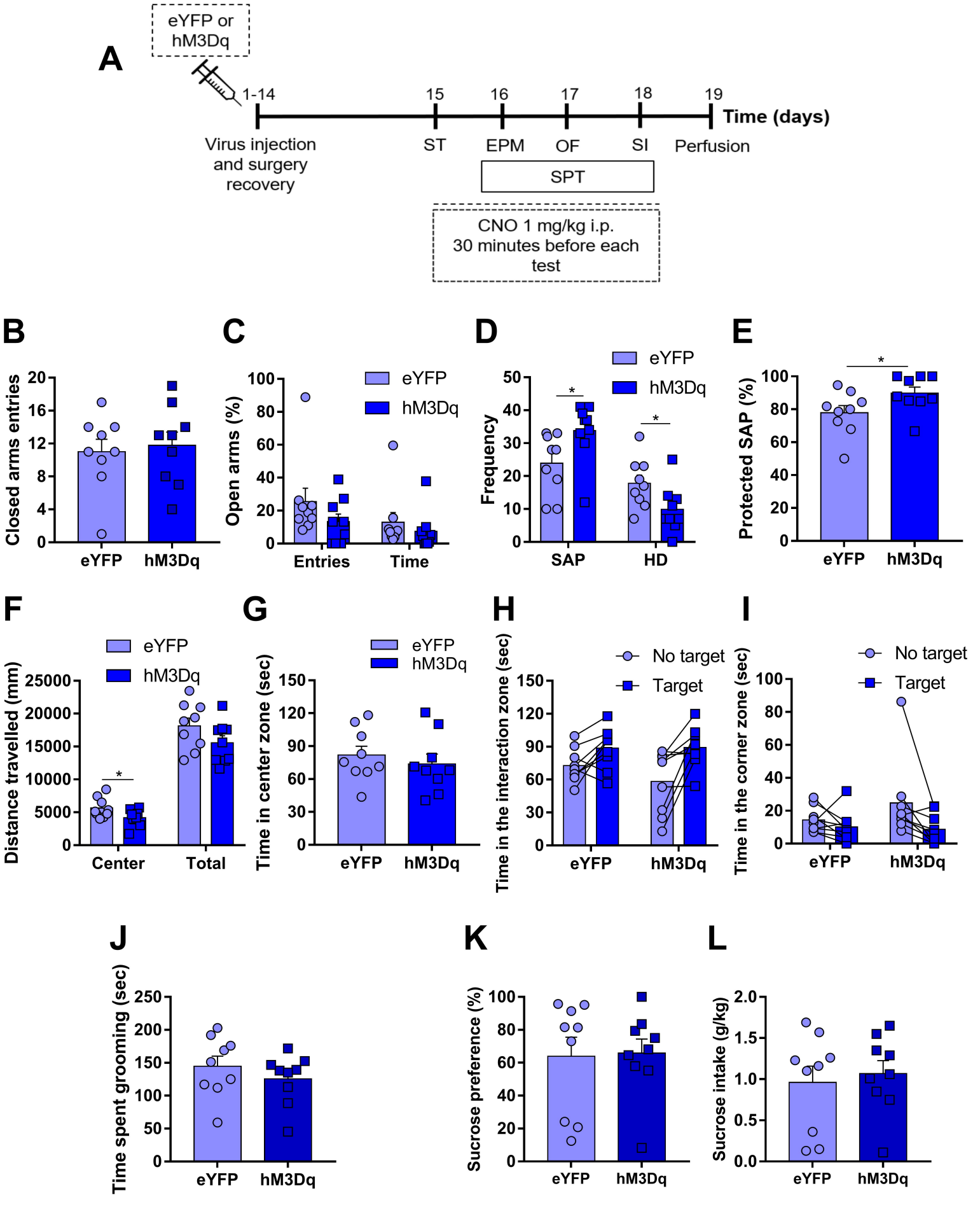
A
eYFP or hM3Dq
1-14
15
16
17
18
19
Time (days)
Virus injection and surgery recovery
ST
EPM
OF
SI
Perfusion
SPT
CNO 1 mg/kg i.p. 30 minutes before each test
B
Closed arms entries
eYFP
hM3Dq
C
Open arms (%)
Entries
Time
D
Frequency
SAP
HD
E
Protected SAP (%)
F
Distance travelled (mm)
Center
Total
G
Time in center zone (sec)
H
Time in the interaction zone (sec)
No target
Target
I
Time in the corner zone (sec)
J
Time spent grooming (sec)
K
Sucrose preference (%)
L
Sucrose intake (g/kg)

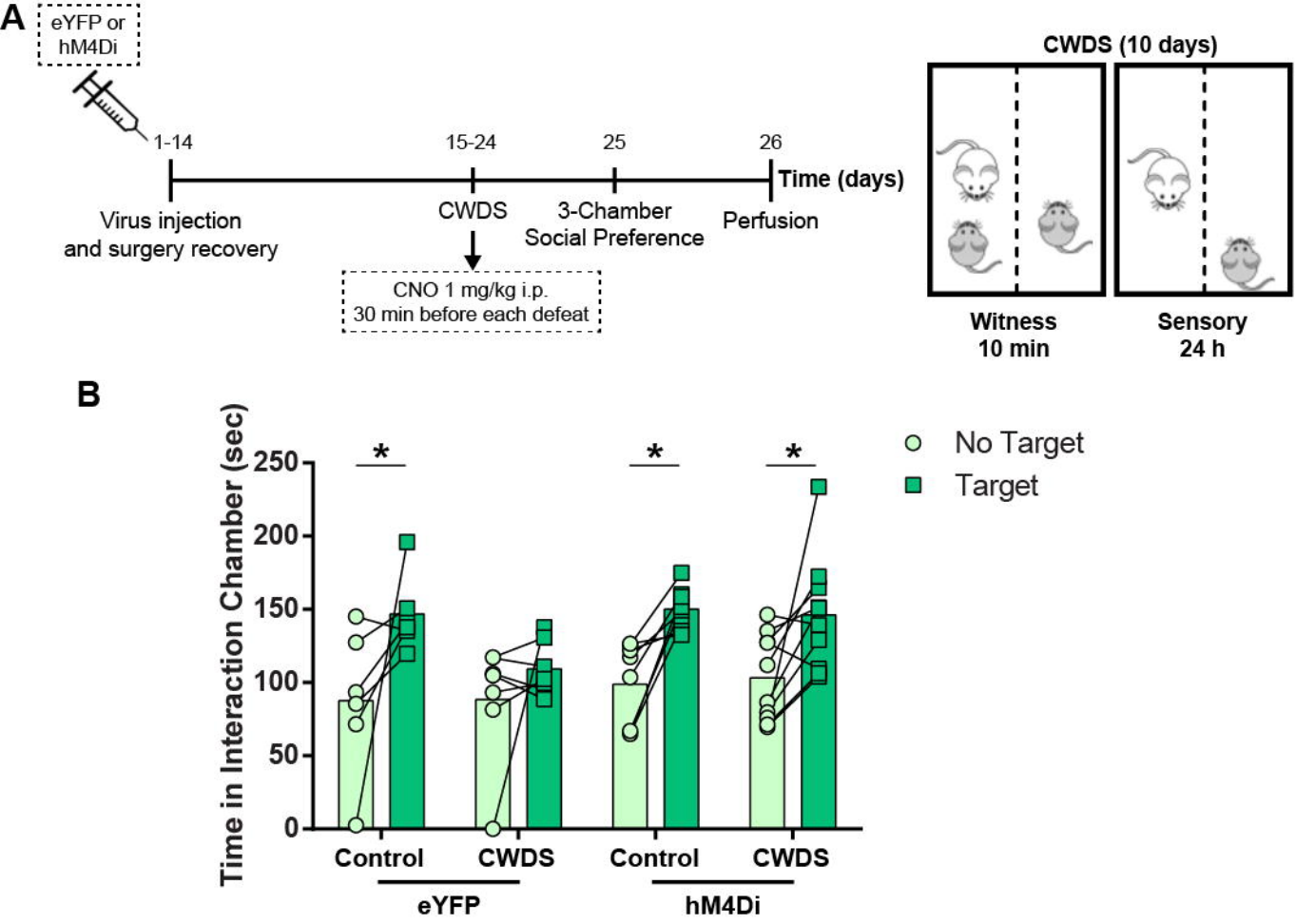
A
eYFP or
hM4Di
1-14
15-24
25
26
Time (days)
Virus injection
and surgery recovery
CWDS
3-Chamber
Social Preference
Perfusion
CNO 1 mg/kg i.p.
30 min before each defeat
CWDS (10 days)
Witness
10 min
Sensory
24 h
B
Time in Interaction Chamber (sec)
250
200
150
100
50
0
*
*
*
No Target
Target
Control
CWDS
Control
CWDS
eYFP
hM4Di

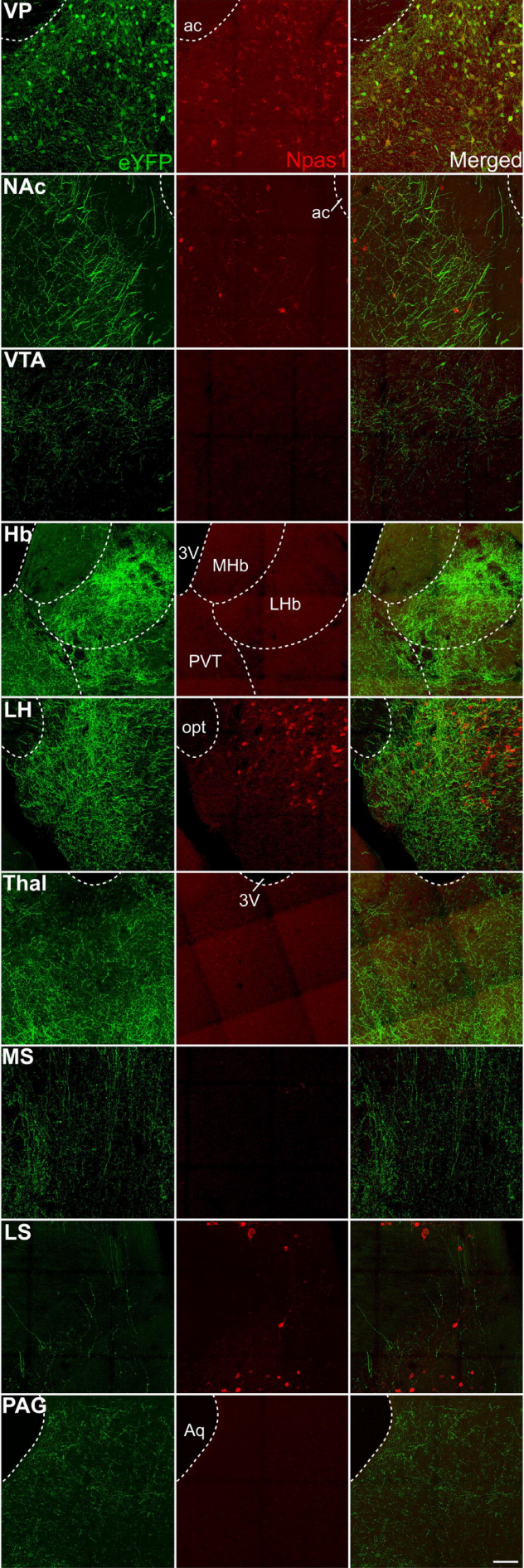
VP
ac
eYFP
Npas1
Merged
NAc
ac
VTA
Hb
3V
MHb
LHb
PVT
LH
opt
Thal
3V
MS
LS
PAG
Aq

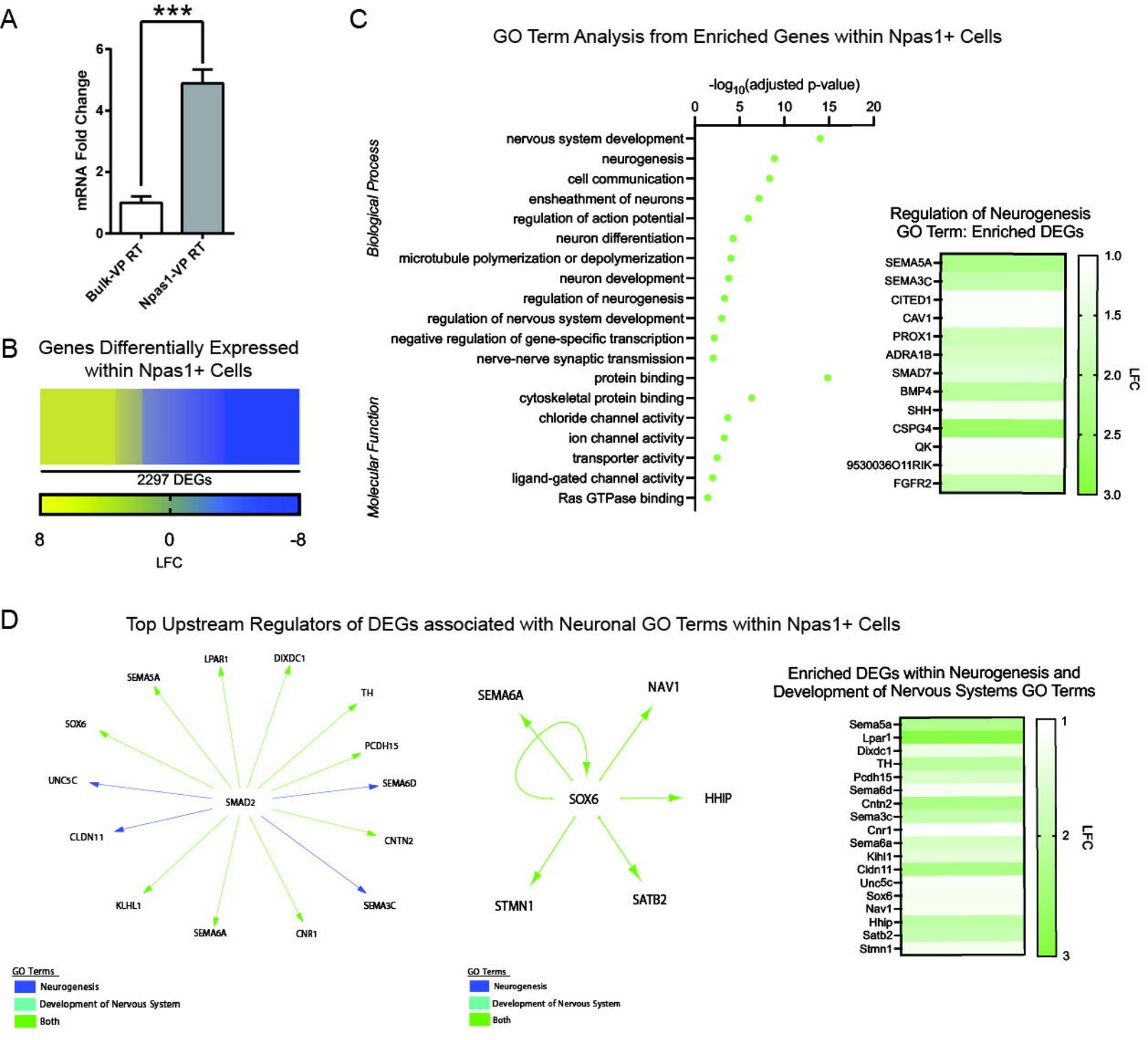
A
***
mRNA Fold Change
0
2
4
6
Bulk-VP RT
Npas1-VP RT
B
Genes Differentially Expressed within Npas1+ Cells
2297 DEGs
8
0
-8
LFC
C
GO Term Analysis from Enriched Genes within Npas1+ Cells
-log10(adjusted p-value)
0
5
10
15
20
Biological Process
nervous system development
neurogenesis
cell communication
ensheathment of neurons
regulation of action potential
neuron differentiation
microtubule polymerization or depolymerization
neuron development
regulation of neurogenesis
regulation of nervous system development
negative regulation of gene-specific transcription
nerve-nerve synaptic transmission
Molecular Function
protein binding
cytoskeletal protein binding
chloride channel activity
ion channel activity
transporter activity
ligand-gated channel activity
Ras GTPase binding
Regulation of Neurogenesis GO Term: Enriched DEGs
SEMA5A
SEMA3C
CITED1
CAV1
PROX1
ADRA1B
SMAD7
BMP4
SHH
CSPG4
QK
9530036O11RIK
FGFR2
1.0
1.5
2.0
2.5
3.0
LFC
D
Top Upstream Regulators of DEGs associated with Neuronal GO Terms within Npas1+ Cells
LPAR1
DIXDC1
SEMA5A
TH
SOX6
PCDH15
UNC5C
SEMA6D
SMAD2
CLDN11
CNTN2
KLHL1
SEMA3C
SEMA6A
CNR1
GO Terms
Neurogenesis
Development of Nervous System
Both
SEMA6A
NAV1
SOX6
HHIP
STMN1
SATB2
GO Terms
Neurogenesis
Development of Nervous System
Both
Enriched DEGs within Neurogenesis and Development of Nervous Systems GO Terms
Sema5a
Lpar1
Dixdc1
TH
Pcdh15
Sema6d
Cntn2
Sema3c
Cnr1
Sema6a
Klhl1
Cldn11
Unc5c
Sox6
Nav1
Hhip
Satb2
Stmn1
1
2
3
LFC